phycology

MDPI

Article

Exposures to UV Radiation Diminish the Positive Effects of Elevated pCO_2 on a Coastal Strain of the Picophytoplankton *Synechococcus*

He Li [1], Yuming Rao [2], Jiayi Cai [1] and Kunshan Gao [2,*]

[1] Jiangsu Key Laboratory of Marine Bioresources and Environment, School of Marine Science and Fisheries, Jiangsu Ocean University, Lianyungang 222000, China
[2] State Key Laboratory of Marine Environmental Science, College of Ocean and Earth Sciences, Xiamen University, Xiamen 361102, China
* Correspondence: ksgao@xmu.edu.cn

Abstract

The cyanobacteria *Synechococcus* spp. are key contributors to marine primary productivity. They are found from equatorial to polar waters where these organisms are exposed to changed levels of pCO_2 and solar ultraviolet radiation (UVR, 280–400 nm). To investigate how elevated pCO_2 modulates the physiological responses of a coastal picocyanobacterium to UVR, *Synechococcus* XM24 was used and acclimated to periodic (90 min per day) near-surface UVR exposure under ambient (418 μatm) and elevated (1000 μatm) pCO_2 conditions for 17 days. Our results indicate that elevated pCO_2 markedly enhanced its specific growth, cellular pigment accumulation (chlorophyll *a*, carotenoids), and particulate organic carbon/nitrogen (POC/PON) quotas in the cells grown under light (without exposure to UVR). However, such stimulatory effects were substantially abolished in UVR-exposed cells. UVR significantly inhibited the effective photochemical quantum yield of photosystem II (PSII) and accelerated PSII damage without a compensatory increase in repair, thereby reducing the repair/damage ratio (r/k) by up to 4-fold. The cells acclimated to the UVR exposures reduced their carbon fixation rate by 56–60% regardless of the pCO_2 levels. In addition, UVR exposure led to drastic reductions in cellular POC and PON content, reflecting a potential energy shift from biomass production towards cellular maintenance. Reduced contents of Chl *a* and carotenoids under the combination of UVR and elevated pCO_2 should be responsible for the reductions in photosynthetic carbon fixation and POC/PON contents. Our results imply that while progressive ocean acidification with increasing pCO_2 can stimulate growth of the coastal *Synechococcus* XM24 under PAR-alone conditions, exposures to UV radiation can diminish such enhancement.

Keywords: CO_2; growth; ocean acidification; photosynthesis; picophytoplankton; *Synechococcus*; ultraviolet radiation

Academic Editor: Feixue Fu

Received: 27 August 2026
Revised: 19 October 2026
Accepted: 25 October 2026
Published: 29 October 2026

Copyright: © 2026 by the authors. Licensee MDPI, Basel, Switzerland. This article is an open access article distributed under the terms and conditions of the Creative Commons Attribution (CC BY) license.

1. Introduction

Synechococcus is a ubiquitous group of picocyanobacteria, with cell diameters ranging from 0.2 to 2 μm. It comprises approximately 15 clades and 28 subclades that are widely distributed from the equator to the poles [1] and contributes approximately 17% of total

ocean primary productivity [2]. Its abundance is predicted to increase by about 10–15% over a century with progressive ocean global changes [3]. Compared to nano- or micro-phytoplankton groups, pico-phytoplankton groups including *Synechococcus* may be more sensitive to ocean climate changes, since they are supposed to be susceptible to solar ultraviolet radiation (UVR, 280–400 nm) and other stressors due to their poor photoprotective capacity [4].

UVR, especially UV-B (280–315 nm), poses a threat to marine life in euphotic zones, despite the curtailed emissions of ozone-depleting substances through the success of the Montreal Protocol [5]. Moreover, progressive global climate-driven changes in cloud cover, aerosols, snow and ice cover, and vertical mixing continue to modulate actual UVR exposure at the ocean surface in different geographical regions [5,6]. Fluctuations in both photosynthetically active radiation (PAR) and UVR regulate phytoplankton physiology, impacting primary production and trophic transfer dynamics in marine ecosystems [7]. UV-B can directly damage biomolecules such as DNA, proteins, and lipids in phytoplankton, causing cellular injury or even death [8,9]. Both UV-B and UV-A (315–400 nm) can also induce reactive oxygen species (ROS), indirectly leading to oxidative damage to cells [10,11]. Nevertheless, some studies have shown that moderate exposures to UVR or UV-A increased primary productivity of phytoplankton assemblages [12–14]. Rapid vertical mixing may also mitigate the UVR inhibition on phytoplankton photosynthesis by balancing UVR-induced damage and cellular repair [15].

To cope with UVR stress, phytoplankton have evolved a suite of defense strategies at behavioral, biochemical, and physiological levels [16,17]. For example, diel vertical migration minimizes exposure to surface UVR, while colony formation provides mutual shading in some taxa [17]. At the cellular level, photoprotective compounds such as mycosporine-like amino acids (MAAs), scytonemin and xanthophylls act as molecular shields by absorbing UVR photons and quenching ROS [18]. In coccolithophores, extracellular coccoliths physically attenuate harmful UV irradiances [19]. Meanwhile, enzymatic ROS scavengers (e.g., superoxide dismutase, catalase) and photolyase-mediated DNA repair are activated to maintain genomic integrity in response to UV-induced damage [18,20]. The efficacy of these protective mechanisms is strongly influenced by other environmental drivers. The diatoms *Chaetoceros gracilis* and *Thalassiosira weissflogii* exhibited diminished photoinhibition at 23 °C during short-term solar UVR exposures compared to those at 18 °C, largely because non-photochemical quenching (NPQ) mediated by xanthophyll pigments operated more efficiently at the higher temperature [21]. Moreover, elevated CO_2 alleviates high PAR and UV stresses in *Dunaliella tertiolecta* by reducing ROS accumulation and enhancing cell nuclear antigen accumulation [22]. Conversely, nutrient limitation imposes critical constraints: nitrogen scarcity suppresses MAA biosynthesis in a coccolithophorid by >60% in the presence of UVR [23], while phosphorus starvation increased susceptibility of *D. tertiolecta* cells to UVR [24].

Marine *Synechococcus* is also highly sensitive to UVR because of its small cell size and limited package effect. UVR can inhibit the productivity and survival of natural picophytoplankton assemblages and *Synechococcus* populations by impairing photosynthesis and damaging cellular components [25–27]. In *Synechococcus* WH8102, UVR caused rapid changes in photosynthetic performance, and the kinetics of inhibition and recovery depended on the balance between PAR and UVR exposure [28]. UV exposure can also induce phycobilisome dismantling in marine *Synechococcus*, reducing light harvesting and energy transfer to PSII [29]. These studies demonstrate that UVR can impair PSII photochemistry, disturb light-harvesting structures, and alter recovery processes in marine *Synechococcus*. Furthermore, studies on other cyanobacteria indicate that UVR can strongly modify or even nearly override the physiological effects of elevated

CO_2 [30], suggesting that CO_2 fertilization effects cannot be evaluated independently of radiation stress.

In contemporary marine systems, progressive ocean acidification (OA) driven by continuous dissolution of anthropogenically emitted CO_2 into seawater is projected to decrease surface ocean pH by about 0.4 units by 2100 under the "business-as-usual" scenario [31]. Moreover, even larger pH drops are anticipated in coastal waters due to the additional CO_2 released by warming-enhanced microbial respiration [32,33]. Numerous studies have shown that the effects of OA on phytoplankton can be positive, negative, or negligible, depending on the balance between CO_2 enrichment and pH decline [34]. For example, the stimulating effects of elevated CO_2 on nitrogen fixation in the diazotroph *Trichodesmium* were outweighed by the inhibitory effect of concurrent seawater pH drop [35]. Yet, elevated pCO_2 enhances photosynthetic quantum yield and growth in several diatoms under low irradiance, whereas it suppresses their growth with increased NPQ under high sunlight [36]. In addition, growth of the diatom *P. tricornutum* at the elevated CO_2 concentration (1000 μatm) increased its NPQ and partially counteracted the harms to PS II (photosystem II) caused by UV-A and UV-B [37]. It is obvious that impacts of OA can be modulated by other stressors [38,39]. Consequently, understanding the ecological consequences of ocean acidification necessitates the interactive or combined effects with other environmental drivers, which is essential for robust predictions of marine ecosystem trajectories under global ocean changes [40].

In surface oceans, *Synechococcus* strains are exposed to multiple, often interacting, environmental factors. Many studies have shown that UVR harms the picophytoplankton by inhibiting its photosynthesis and damaging DNA, ultimately leading to cell death [25,26]. Other studies have demonstrated that *Synechococcus* strains may display distinct responses to ocean acidification (OA) and changing light levels. For example, *Synechococcus* WH7803 (oceanic strain) grew faster under OA due to increased CO_2 availability only under growth-limited light levels [41], whereas the combination of over-saturating light intensities and OA inhibited the growth and photosynthesis of *Synechococcus* CB0101 (coastal strain) due to synergetic impacts of photoinhibition and acidic stress [42]. Similarly, temperature and irradiance can interactively regulate the physiology of marine *Synechococcus* WH7803, further emphasizing that its responses to global-change drivers are context dependent [43]. While individual effects of OA and UVR have been documented separately for some *Synechococcus* strains, little has been documented on the combined impacts of OA and UVR on the physiological performance of coastal *Synechococcus* strains. Coastal ecotypes experience frequent fluctuations in both carbonate chemistry [32] due to eutrophication and solar radiation [44] due to terrestrial inputs, tides, mixing, and variable weather conditions, making them particularly relevant for studying interactive effects of UV and pH.

Understanding whether OA-induced benefits persist under realistic UVR exposure regimes is essential for projecting net responses of picophytoplankton to future global ocean changes. Based on previous knowledge about its response to UVR or OA, we hypothesize that the response of *Synechococcus* to ocean acidification can be modulated by exposures to UVR. To test this hypothesis, we selected the coastal strain *Synechococcus* XM24, isolated from the southern East China Sea and representative of a typical coastal ecotype that experiences frequent environmental fluctuations. We used this strain to (1) quantify the individual effects of elevated pCO_2 and periodic UVR exposure on growth, photochemical performance, and carbon/nitrogen assimilation, and (2) determine whether the effect of elevated pCO_2 is altered by UVR-induced PSII damage and repair dynamics. In this study, we found that this strain benefited less from CO_2 rise when exposed to periodic UVR exposures in terms of its growth, photosynthetic performance and particulate matter production.

https://doi.org/10.3390/phycology6040118

2. Materials and Methods

2.1. Culture Conditions and Experimental Design

The *Synechococcus* strain XM24 was isolated from Wuyuan Bay (Xiamen, Fujian Province, China) and maintained in autoclaved artificial seawater enriched with SN medium [45]. Cultures were grown in 500 mL polycarbonate bottles at 23 ± 0.5 °C under about 150 μmol photons m^{-2} s^{-1} of PAR with 12 h:12 h light and dark cycles in an incubator (GXZ280, Jiangnan, Ningbo, China). Three independent replicate cultures were maintained for each treatment by semi-continuous dilution (every 2 days) to keep stable carbonate chemistry and keep cells in the exponential growth phase [46]. To achieve the two pCO_2 levels, the culture medium was pre-equilibrated with 0.2-μm-filtered outdoor ambient air (418 μatm, AC; represents current atmospheric CO_2 conditions) and elevated CO_2 (1000 μatm, HC; represents the end-of-century "business-as-usual" scenario), respectively. The elevated pCO_2 level was generated by mixing air and pure CO_2 using a commercial CO_2 enrichment device (CE100D, Ruihua, Wuhan, China). Cultures were continuously aerated with the target pCO_2 levels at 0.2 L min^{-1}. The dilution ratio was adjusted based on the growth rate to keep final densities <5 × 10^6 cells mL^{-1} throughout the acclimation period.

For the periodic UV exposures, the *Synechococcus* cells were transferred into quartz tubes (volume ~500 mL) and exposed to a solar simulator (Sol 1200 W, Heraeus, Marstinstried, Germany) for approximately 90 min daily around mid-photoperiod [23]. During the exposure, the quartz tubes were placed horizontally in a temperature-controlled water bath (23 ± 0.5 °C, the same temperature level as in the culture) and their positions were periodically exchanged to ensure uniform light exposure. The quartz tubes were wrapped with two different cut-off foils to obtain two radiation treatments: (1) PAR alone treatment, wrapped with 395 nm cut-off film transmitting irradiance above 395 nm (Ultraphan UV Opak, Digefra); (2) PAR+UVR treatment, wrapped with 295 nm cut-off film transmitting irradiance above 295 nm (Ultraphan, Digefra). The cells were exposed for 90 min with PAR of ~1500 μmol photons m^{-2} s^{-1} (ca 326 W m^{-2}), UV-A of 33 W m^{-2} (315–395 nm) and UV-B of 3.6 W m^{-2} (295–315 nm), the values of which were close to incident solar irradiances at noon near the sea surface in Xiamen (Fujian province, China) for the subtropical regions (Figure S1). Such radiation treatments, designed to represent a short-term near-surface exposure scenario, were run daily until the cells had acclimated for about 15 generations. Apart from the exposures, the cells were maintained under the growth PAR (150 μmol photons m^{-2} s^{-1}), with the same temperature as mentioned above.

2.2. Carbonate Chemistry Parameters

The pH_{NBS} was measured using a high-precision pH meter (Orion 2 STAR, Thermo Scientific, Waltham, MA, USA), which was three-point calibrated with NBS (National Bureau of Standards) buffer. Total alkalinity (TA) was determined by Gran acidimetric titration with a TA analyzer (AS-ALK+, Apollo SciTech, Newark, DE, USA). Other parameters of the carbonate system were calculated using CO2SYS software v14 based on the temperature, salinity, pH_{NBS} and TA determined from the samples (Table 1).

Table 1. Carbonate chemistry parameters in the semi-continuous cultures of *Synechococcus* XM24 with or without exposure to UVR under ambient (AC, 418 μatm) and elevated (HC, 1000 μatm) CO_2 levels. The values of pH_{NBS} and total alkalinity (TA) were measured and other carbonate chemistry parameters were obtained by using the CO2SYS. Values are means ± SDs of triplicate cultures (n = 3). Different superscripted letters indicate significant ($p < 0.05$) differences among the treatments.

		pH_{NBS}	TA (μM)	DIC (μM)	CO_2 (μM)	HCO_3^- (μM)	CO_3^{2-} (μM)
PAR	AC	8.17 ± 0.02 [a]	2271.8 ± 6.7 [a]	1940.3 ± 13.9 [a]	12.7 ± 0.6 [a]	1761.0 ± 17.7 [a]	166.6 ± 4.5 [a]
	HC	7.82 ± 0.01 [b]	2295 ± 6.7 [a]	2111.0 ± 6.3 [b]	32.2 ± 0.4 [b]	1994.5 ± 6.1 [b]	84.3 ± 1.1 [b]
UVR	AC	8.15 ± 0.02 [a]	2211.2 ± 15.6 [a]	1895.3 ± 16.2 [a]	13.1 ± 0.7 [a]	1726.9 ± 18.5 [a]	155.2 ± 6.3 [a]
	HC	7.83 ± 0.00 [b]	2233.7 ± 7.8 [a]	2048.9 ± 7.3 [b]	30.8 ± 0.1 [b]	1935.1 ± 6.8 [b]	83.1 ± 0.5 [b]

2.3. Specific Growth Rate

Samples of each replicate were filtered and measured using a flow cytometer (CytoFLEX S, Beckman Coulter, Brea, CA, USA) and *Synechococcus* cell concentrations were estimated [47]. The specific growth rate was calculated according to the difference in cell densities between the two consecutive dilutions as follows:

$$\mu = (\ln N - \ln N_0)/(t - t_0),$$

where N and N_0 are the cell densities at the times t and t_0, respectively.

2.4. Pigment and UVAC Content

The collected cells of *Synechococcus* following different radiation treatments were filtered onto GF/F filters (Ø 25 mm, Whatman, Maidstone, UK) for analysis of chlorophyll *a* (Chl *a*) and carotenoids (Car). The filters were extracted in absolute methanol at 4 °C for 24 h in darkness. After centrifugation at 8000× *g* (Universal 320R, Hettich, Kirchlengern, Germany) for 10 min, the supernatant was scanned for absorbance values from 200 to 800 nm with a UV spectrophotometer (DU800, Beckman, Dutchess County, NY, USA). The concentrations of Chl *a* and Car were calculated according to the equations as follows [48,49]:

$$\text{Chl } a\ (\mu g\ mL^{-1}) = 12.9447 \times (A_{665} - A_{750});$$

$$\text{Car } (\mu g\ mL^{-1}) = [1000 \times (A_{470} - A_{750}) - 2.86 \times (\text{Chl } a)]\ /\ 221.$$

The key spectral characteristic of UV-absorbing compounds (UVACs) is characterized by absorption peaks situated between 310 and 340 nm [50]. However, in this study, the *Synechococcus* strain did not exhibit a distinct characteristic absorption peak within the UV band (Figure S3). We note that methanol extraction is less sensitive than HPLC and cannot definitively establish the absence of MAAs or scytonemin. Therefore, this result should be regarded as indirect evidence only. Future studies using a more sensitive method such as HPLC are needed to verify whether trace UVACs are present in this strain.

2.5. Chlorophyll a Fluorescence

In vivo chlorophyll *a* fluorescence parameters were measured using a Multi-Color PAM fluorometer (Multi-Color PAM, Heinz Walz GmbH, Effeltrich, Germany). The effective photochemical quantum yield (Φ_{PSII}) of samples was measured at the actinic light similar to the growth light level. Rapid light curves for the cells grown under different treatments were determined at 13 actinic light intensities, ranging from 0 to 2855 μmol photons m^{-2} s^{-1}, with a duration of 20 s at each step (Figure S2). The light-harvesting

efficiency (a), maximum electron transport rate ($rETR_{max}$), and light saturation point (I_k) were obtained by fitting the equation of Eilers and Peeters [51]:

$$rETR = PAR/(a \times PAR^2 + b \times PAR + c),$$

where a, b, and c are the model parameters.

To determine the photochemical responses of *Synechococcus* to UVR during the exposures, subsamples of *Synechococcus* were dispensed to quartz tubes under the corresponding radiation treatments. The yields of samples were recorded at timepoints of 0, 3, 6, 9, 12, 15, 20, 25, 30, 40, 50, and 60 min. The repair (r) and damage (k) rates during the periods were fitted using the Kok model [52]:

$$P/P_{initial} = \frac{r}{r+k} + \frac{k}{r+k} e^{-(r+k)\times t},$$

where the $P_{initial}$ and P were the yield values at the beginning and at exposure time t.

2.6. Determination of Photosynthetic Carbon Fixation

Carbon fixation rates of *Synechococcus* cells were determined as previously reported using the ^{14}C method [14]. After the exposure to UVR, about 20 mL volumes of samples were placed in 25 mL borosilicate bottles and inoculated with 5 μCi of labeled $NaH^{14}CO_3$ (ICN Radiochemicals, Costa Mesa, CA, USA), and were then maintained under the same pCO_2 level and growth PAR without UVR in the incubator. After 1 h of incubation, the cells were immediately filtered onto GF/F filters under low light, and the filters were fumed with HCl overnight to expel non-fixed ^{14}C as $^{14}CO_2$, followed by drying at 60 °C for 5 h to remove residual acid. To determine the radioactivity, the samples were immersed in 4 mL of scintillation solution (Hisafe 3, Perkin-Elmer, Waltham, MA, USA) for 2 h, and then measured with a liquid scintillation counter (Tri-Carb 2800TR, PerkinElmer, Shelton, CT, USA). Because incubations were conducted without UVR, these measurements represent post-exposure photosynthetic carbon fixation rather than direct UVR inhibition during the assay.

2.7. Measurements of Particulate C and N

To measure cellular particulate organic carbon (POC) and nitrogen (PON), *Synechococcus* cells were harvested onto pre-combusted (450 °C for 6 h) GF/F filters following the UV exposures and stored at −80 °C until analysis. After acid fuming with HCl at room temperatures for 12 h and drying at 60 °C to remove inorganic carbon, the filters were packed into cups and analyzed with a CHNS/O elemental analyzer (Vario EL cube, Elementar, Langenselbold, Germany).

2.8. Data Analysis

All data are presented as the means ± SD of three independent cultures. Two-way analysis of variance (ANOVA) was used to test the differences for pCO_2 concentrations, UV treatments and their interactions among treatments ($p < 0.05$). A Tukey post hoc (Tukey HSD) test was used to analyze the differences between pCO_2 concentrations and/or UV treatments.

3. Results

3.1. Specific Growth Rate

The specific growth rates of *Synechococcus* cells acclimated to periodic exposure to UVR under the AC and HC were 0.58 ± 0.03 and 0.64 ± 0.04, respectively. Two-way ANOVA showed that pCO_2 and UVR had significant individual effects on specific growth rate ($p = 0.004$, $p < 0.001$), whereas their interaction was not significant ($p = 0.576$). These

growth rates were significantly lower, correspondingly by about 24% under either pCO_2 level compared to the cells grown under the PAR alone (Figure 1, $p < 0.001$, $p < 0.001$). The elevated pCO_2 significantly enhanced the specific growth rates ($p < 0.001$), by 10.7% compared to the AC-under-PAR-alone condition, but had no effect on cell growth with periodic UVR exposures ($p = 0.163$). Thus, elevated pCO_2 stimulated growth only in the absence of UVR.

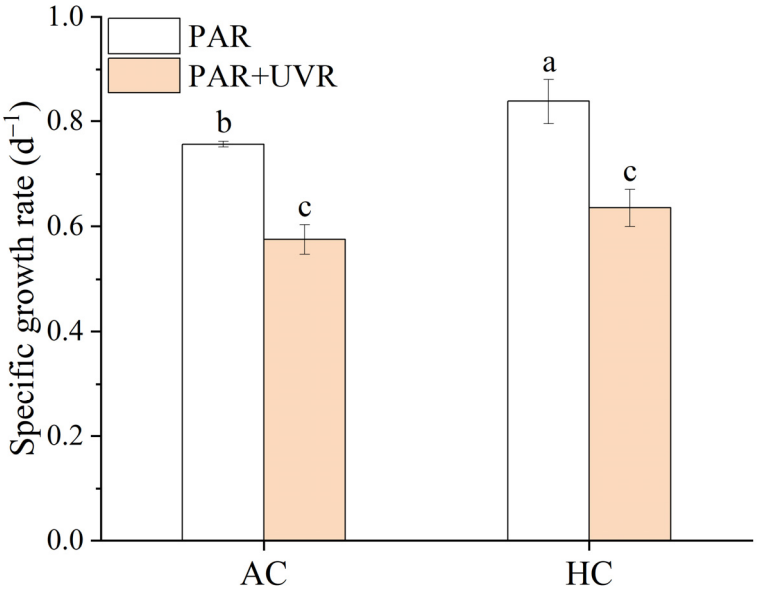


Figure 1. The specific growth rates of *Synechococcus* XM24 acclimated for 14~20 generations to the growth conditions with or without periodic exposures to UVR under the two CO_2 levels (AC: 418 μatm, HC: 1000 μatm). Values are the mean ± SD for triplicate cultures ($n = 3$). Different letters indicate significant ($p < 0.05$) differences among the treatments.

3.2. Pigment Content

Two-way ANOVA revealed significant individual and interactive effects of CO_2 and UVR on Chl *a* content ($p = 0.002$, $p < 0.001$, $p = 0.015$, respectively). Similarly, significant individual and interactive effects were observed for carotenoids ($p < 0.001$, $p < 0.001$, $p = 0.005$). Compared to AC, the Chl *a* and carotenoid contents of HC-acclimated cells were significantly increased by 34.8% and 39.2% in the PAR-only cultures, respectively (Figure 2A,B, $p = 0.003$, $p = 0.001$). +UVR treatment decreased the cellular Chl *a* by 20.5% ($p = 0.013$) and carotenoids by 30.7% ($p = 0.003$) in the *Synechococcus* cells grown under AC. In contrast, +UVR treatment decreased Chl *a* and carotenoids of the cells grown under the HC by 35.9% and 44.9% ($p < 0.001$, $p < 0.001$), respectively (Figure 2A,B). Nevertheless, the cellular Car:Chl *a* ratios ranged from 0.94 to 1.11, being significantly lower in the cells exposed to UVR treatment (Figure 2C, $p < 0.001$). These results indicate that elevated pCO_2 increased pigment investment under PAR alone, but UVR abolished this benefit and reduced photoprotective capacity.

3.3. Photochemical Performance

The effective quantum yield of *Synechococcus* was significantly affected by UVR and by the interaction between UVR and CO_2 ($p < 0.001$, $p = 0.048$). The yield of cells exposed to UVR decreased significantly by 19.4% and 12.8% under AC and HC conditions, respectively (Figure 3A, $p < 0.001$), while the elevated CO_2 did not significantly affect it ($p = 0.693$). The apparent light use efficiency (α) and the maximal electron transport ($rETR_{max}$), which were significantly affected only by UVR ($p < 0.001$, $p < 0.001$), showed similar trends

with the yield of the cells in +UVR treatment, declining significantly regardless of the pCO_2 levels (Figure 3B,C). Thus, UVR was the dominant driver of photochemical inhibition.

During the short-term PAR+UVR exposure, the relative photochemical efficiency of *Synechococcus* cells declined significantly within 15 min and thereafter leveled off in the cells grown under all treatments (Figure 4). Regardless of pCO_2 levels, the cells grown under PAR alone had a smaller decrease in the yield than that in the presence of UVR. However, +UVR treatment significantly reduced it by 42.4% under AC and by 47.4% under HC, respectively, in terms of the leveled lowest values ($p < 0.001$, $p < 0.001$). The damage (k, min^{-1}) and repair (r, min^{-1}) rates of the PSII derived from the exponential decay of the relative quantum yield in the *Synechococcus* cells showed that +UVR treatment enhanced the damage and suppressed the repair (Figure 5A,B). Two-way ANOVA showed that the damage rate was significantly increased by the interaction between CO_2 and UVR ($p < 0.001$). The damage rates in the presence of UVR were 0.14 and 0.18 min^{-1} in the AC and HC conditions, respectively, about 4 times higher than that in the cells without exposure to UVR (PAR alone) (Figure 5A, $p < 0.001$, $p < 0.001$). The repair rates of UVR-exposed cells were both about 0.12 min^{-1} in the AC and HC-grown cells, with no significance compared to that of the PAR treatment (Figure 5B, $p = 0.733$, $p = 0.381$). Accordingly, the ratios of r to k showed significantly lower values in +UVR treatments compared with PAR-alone conditions (Figure 5C, $p < 0.001$, $p < 0.001$). On the other hand, the elevated CO_2 levels significantly decreased the r/k ratios in the cells with +UVR treatment ($p = 0.012$). These data indicate that UVR increased PSII damage without a compensatory increase in repair, thereby reducing the repair-to-damage balance.

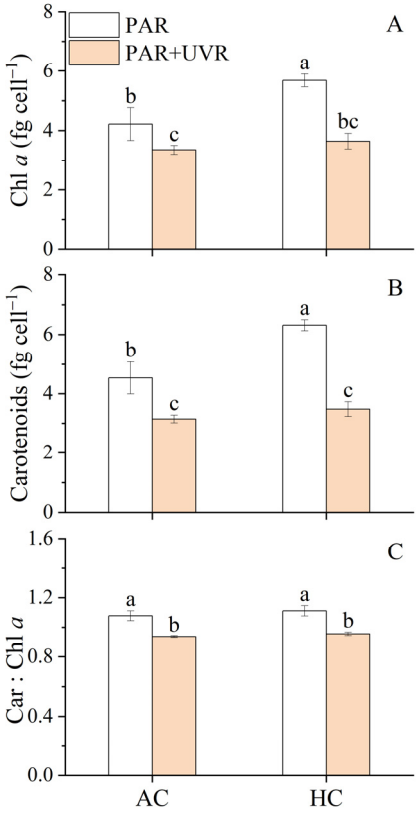


Figure 2. The contents of chlorophyll *a* (Chl *a*) (**A**), carotenoids (Car) per cell (**B**), and Car:Chl *a* ratio (fg:fg) (**C**) in *Synechococcus* XM24 acclimated for 14~20 generations to the growth conditions with or without periodic exposures to UVR under the two CO_2 levels (AC: 418 μatm, HC: 1000 μatm).

https://doi.org/10.3390/phycology6040118

Values are the mean ± SD for triplicate cultures ($n = 3$). Different letters indicate significant ($p < 0.05$) differences among the treatments.

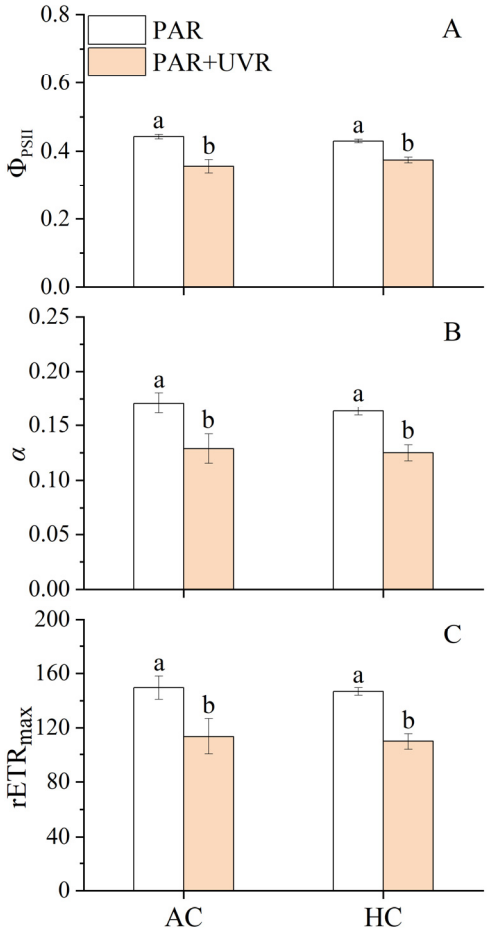


Figure 3. The effective photochemical quantum yield (Φ_{PSII}) (**A**), photosynthetic light-harvesting efficiency (α) (**B**), and maximum electron transport rate ($rETR_{max}$) (**C**) in *Synechococcus* XM24 acclimated for 14~20 generations to the growth conditions with or without periodic exposures to UVR under the two CO_2 levels (AC: 418 μatm, HC: 1000 μatm). The fluorescence parameters were measured immediately after UVR exposure, and the α and $rETR_{max}$ were derived from rapid light curves (see Figure S1). The AC-PAR treatment has been designated as the control group. Values are the mean ± SD for triplicate cultures ($n = 3$). Different letters indicate significant ($p < 0.05$) differences among the treatments.

3.4. Carbon Fixation

The carbon fixation rate was significantly affected only by UVR ($p < 0.001$), whereas CO_2 and the interaction showed no significant effects ($p = 0.146$, $p = 0.233$). While the *Synechococcus* cells grown under HC exhibited 14.8% higher photosynthetic carbon fixation than that at AC level under PAR-alone conditions, such difference was nonsignificant (Figure 6, $p = 0.247$). It appears that HC treatment did not result in any enhancement of carbon fixation even in the cells exposed to +UVR treatment ($p = 0.996$). However, periodic exposures to UVR decreased the carbon fixation by 56.0% and 60.3% under AC and HC conditions, respectively (Figure 6, $p < 0.001$, $p < 0.001$).

3.5. Cellular Organic C and N Quotas

The particulate organic carbon (POC) content was significantly affected by UVR and the interaction with CO_2 (p = 0.009, p = 0.048). Elevated pCO_2 significantly raised the cellular POC by 24.2% (p = 0.048) in the *Synechococcus* cells grown under PAR-alone conditions, but resulted in a nonsignificant effect (p = 0.999) on it in those exposed to +UVR (Figure 7A). The particulate organic nitrogen (PON) content was significantly affected by CO_2, UVR, and their interaction ($p < 0.001$, $p < 0.001$, $p = 0.034$). PON increased by 37.6% ($p < 0.001$) in the PAR-alone cultures and by 19.5% (p = 0.040) in the +UVR cultures (Figure 7B). The +UVR treatment significantly decreased the POC by 24.6% (p = 0.015) and the PON by 32.2% ($p < 0.001$) under the HC conditions, respectively. However, the +UVR condition only significantly decreased the PON content by 21.8% in the cells grown under the AC treatment (p = 0.033). The cellular C:N ratios ranged from 5.71 to 7.63, with a significant increase by 20.5% (p = 0.040) under AC and by 11.2% (p = 0.406) under HC. It appears that +UVR treatment increased C:N ratios, though the effect was not significant under HC (Figure 7C). These results suggest that UVR shifted cellular resources away from biomass accumulation toward maintenance and repair.

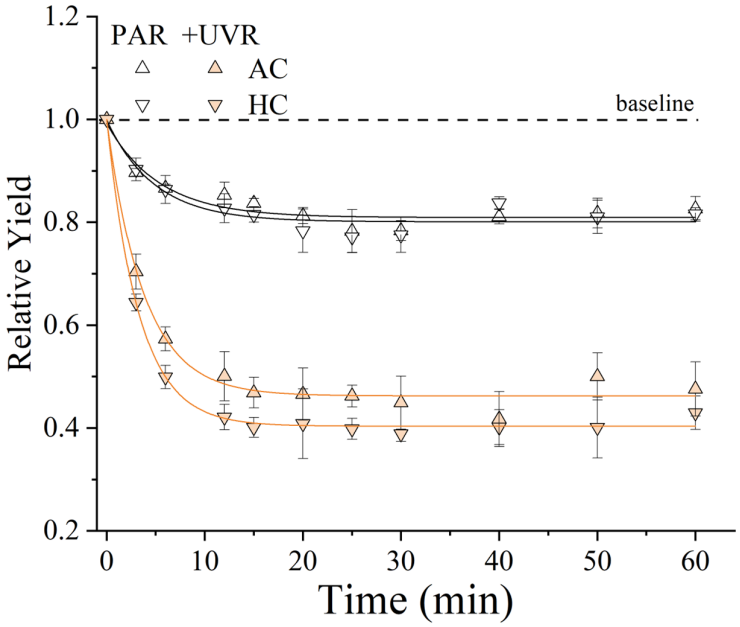


Figure 4. Changes in relative effective PSII quantum yield of *Synechococcus* XM24 acclimated for 14~20 generations grown under different conditions when exposed to PAR and UVR (PAR + UV-A + UV-B) under a solar simulator for 60 min. Relative yield was calculated as $P/P_{initial}$, where P is the effective quantum yield at the beginning of exposure and $P_{initial}$ is the yield at exposure time t. AC and HC indicate ambient (418 µatm) and elevated pCO_2 (1000 µatm), respectively. Upward triangles denote AC conditions; downward triangles denote HC conditions; open symbols indicate PAR-only conditions; orange shading indicates the presence of UVR. Values are the mean ± SD for triplicate cultures (n = 3).

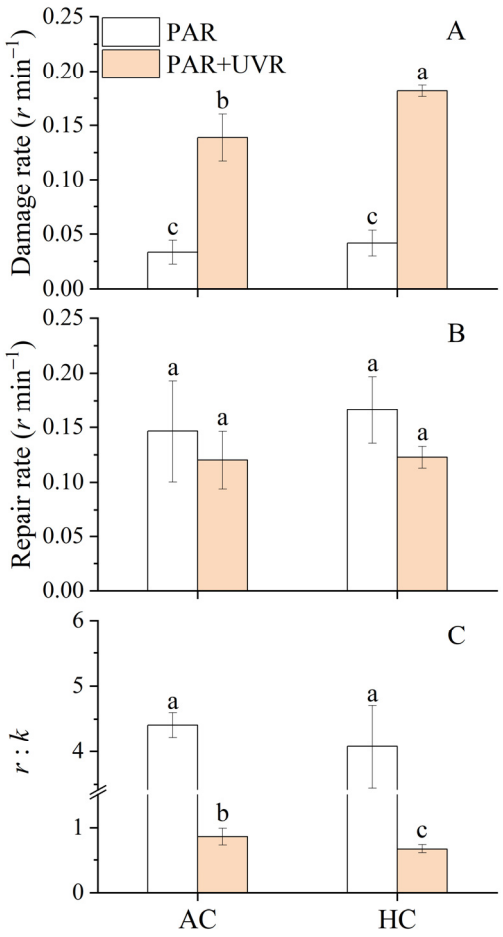


Figure 5. The damage (k, min^{-1}) (**A**), repair rates (r, min^{-1}) (**B**), and r:k ratio (**C**) derived from the relative yield decline curves in Figure 4 of *Synechococcus* XM24 acclimated for 14~20 generations to the growth conditions with or without periodic exposures to UVR under the two CO_2 levels (AC: 418 µatm, HC: 1000 µatm). Values are the mean ± SD for triplicate cultures (n = 3). Different letters indicate significant ($p < 0.05$) differences among the treatments.

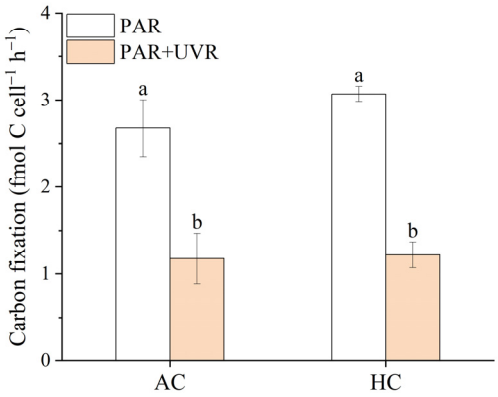


Figure 6. Photosynthetic carbon fixation of *Synechococcus* XM24 per cell acclimated for 14~20 generations to the growth conditions with or without periodic exposures to UVR under the two CO_2 levels (AC: 418 µatm, HC: 1000 µatm). The measurement was carried out immediately following

the UVR exposure. Values are the mean ± SD for triplicate cultures (n = 3). Different letters indicate significant ($p < 0.05$) differences among the treatments.

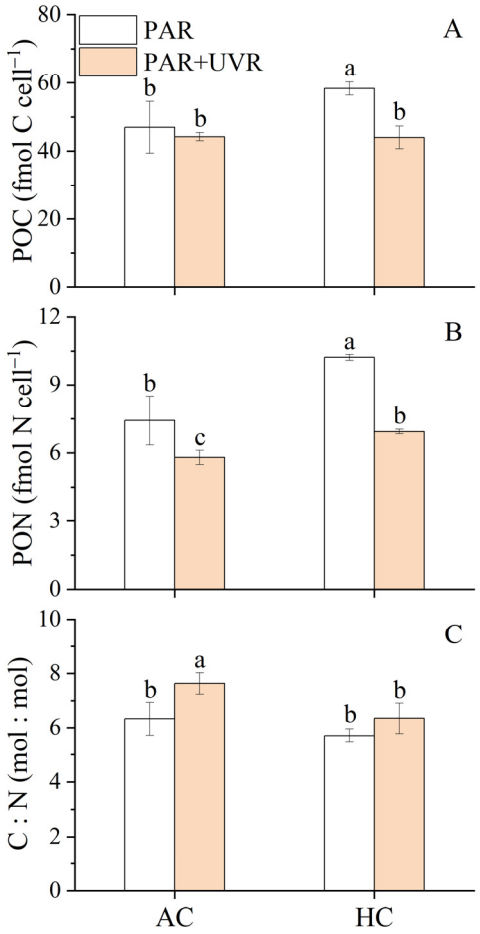


Figure 7. The particulate organic carbon (POC) (**A**), particulate organic nitrogen (PON) (**B**) per cell, and cellular C:N ratio (mol:mol) (**C**) in *Synechococcus* XM24 cells acclimated for 14~20 generations to the growth conditions with or without periodic exposures to UVR under the two CO_2 levels (AC: 418 μatm, HC: 1000 μatm). Samples were harvested after acute UVR exposure. Values are the mean ± SD for triplicate cultures (n = 3). Different letters indicate significant ($p < 0.05$) differences among the treatments.

4. Discussion

Our findings show that periodic UV exposures significantly depressed the growth and photosynthetic carbon fixation of *Synechococcus* XM24, regardless of pCO_2 levels. Elevated pCO_2 (HC) stimulated synthesis of Chl *a* and carotenoids, ultimately enhancing carbon fixation and growth of the *Synechococcus* in the absence of UV exposure. However, such enhancements were substantially diminished or abolished in the cells acclimated to the UVR exposure. The UVR treatment inhibited photosynthesis of *Synechococcus* mainly by increasing PSII photodamage without a compensatory enhancement of repair, thereby lowering the repair-to-damage balance and counteracting the beneficial effects of elevated pCO_2 projected for the end of this century.

Most cyanobacteria as well as other phytoplankton groups possess mechanisms to cope with UVR stress, such as synthesizing and accumulating UV-absorbing compounds

(UVACs) that enable them to effectively resist UV-induced damages [53,54]. However, picophytoplankton like *Synechococcus* appear unable to accumulate these compounds and are highly sensitive to UV exposure [55–57]. In the present study, the methanol extraction assay did not detect a distinct UVAC absorption peak in *Synechococcus* XM24 (Figure S3). Although this method is less sensitive than HPLC and cannot conclusively prove the absence of UVACs, the result may contribute to the observed UV sensitivity (Figure 5). The rapid decline in the effective quantum yield within 15 min of UVR exposures (Figure 4) reflects immediate photoinhibitory stress. UV-B radiation primarily impairs the Mn_4Ca catalytic site of the water-oxidizing complex in PSII, with additional effects on the quinone electron acceptors and tyrosine donors [11]. This heightened damage susceptibility also likely results from direct UV-B absorption by PSII components and UV-A/UV-B-induced ROS production, which accelerates D1 subunit degradation [11,58]. The PSII damage-repair analysis indicates that UVR primarily increased the damage rate rather than clearly suppressing repair (Figure 5). Repair rates did not differ significantly among treatment; thus the lower r/k ratio under UVR mainly reflects enhanced photodamage without a compensatory increase in repair capacity. This interpretation is consistent with previous studies showing that UVR rapidly inhibits photochemical efficiency in *Synechococcus* and other cyanobacteria through damage to PSII reaction centers, D1 protein turnover, and disruption of photosynthetic energy transfer [28,29]. In addition, the higher PSII damage rate (k) observed under HC than under AC in the presence of UVR suggests that elevated pCO_2 and the associated lower pH may increase the susceptibility of PSII to UVR. One possible explanation is that acidification could modify cellular redox balance, proton homeostasis, or the stability of PSII components, thereby increasing susceptibility to UV-induced photodamage.

Synechococcus strains have developed CO_2 concentrating mechanisms (CCMs) to meet substantial CO_2 requirements for carboxylation [59]. Nevertheless, elevating pCO_2 to 1000 μatm enhanced its growth, and Chl *a* and POC contents (Figures 1, 2 and 7), although the increases in photosynthetic carbon fixation rates were not significant (Figure 6). Integrated carbon fixation over the entire photoperiod, differences in respiratory carbon loss, dissolved organic carbon release, or allocation of recently fixed carbon into particulate biomass could all contribute to the observed mismatch between instantaneous carbon fixation (only 1 h in this study) and accumulated POC/growth responses. Because CCM activity, bicarbonate transport, carbonic anhydrase activity, and CCM-related gene or protein expression were not directly measured in this study, we interpret the potential reduction in CCM energetic cost under elevated pCO_2 as a plausible explanation rather than a demonstrated mechanism. In small picocyanobacterial cells, the absolute energetic saving from CCM down-regulation may be limited, and other processes, such as reduced photorespiration, altered respiratory carbon loss, or dissolved organic carbon release, may also contribute to the observed increases in growth and POC under HC conditions (Figure 1) [60]. Therefore, the HC-induced enhancement observed here should be interpreted as an integrated physiological response to increased CO_2 availability and decreased pH, rather than as direct evidence of CCM down-regulation. This physiological response was also reflected in the increment in the contents of Chl *a* and POC (Figures 2A and 7A), indicating enhanced investment in the light-harvesting apparatus to capture more light quanta [61]. These findings align with CO_2-stimulated synthesis of pigments and expression of light-harvesting proteins in diatoms [62,63]. However, these promoting effects induced by the elevated pCO_2 disappeared in UV-exposed cells. Nevertheless, the nonsignificant changes in the effective photochemical efficiency and electron transport rate of PSII in the HC-grown cells (Figure 3) could be attributed to the quenching of PSII complexes during the state transition, a process that may serve to mitigate the potential excessive light energy [64].

Apart from the light-harvesting role in photosynthesis, carotenoids are known to serve as antioxidants to scavenge free radicals under oxidative stress induced by UVR [65] and acidic stress (pH drop) [66]. In this work, under PAR-only conditions, elevated pCO_2 significantly increased cellular carotenoid content together with Chl *a* (Figure 2), suggesting that improved carbon availability may have promoted investment in pigment synthesis and photosynthetic apparatus development. Moreover, carotenoids were significantly reduced in UV-exposed cells along with decreased ratios of Car to Chl *a*, reflecting diminished photoprotective capacity. Mechanistically, binding with free radicals may bleach carotenoids, thereby decreasing their content [67]. The reduced Car:Chl *a* ratio would further weaken photoprotection and increase the vulnerability of PSII to subsequent UVR exposure. While phycobiliproteins were not directly measured, there is a possibility that phycobilisomes were damaged in strain XM24, since previous studies have shown UV-induced phycobilisome dismantling in marine *Synechococcus* [29]. Direct quantification of phycobiliproteins and phycobilisome integrity should be prioritized in future work.

Previously, *Synechococcus* sp. CB0101 cells acclimated to excessive light and OA treatment (the same pCO_2 level as in this work) showed decreased photosynthesis and growth [42]. Although different strains may respond differentially to acidic and light stresses, synergistic impacts of UVR and pH drop likely contributed to the diminished enhancement of growth and decline in photochemical performance (Figure 3A–C). Reduced photosynthetic electron transport under UVR stress [68] and UV-induced damage to the D1 protein of PSII [69] may also be responsible for the diminished effects of OA on *Synechococcus*, though damage to DNA and proteins cannot be ruled out. The most dramatic impact that photosynthetic carbon fixation was inhibited by 56–60% (Figure 6) suggests UVR may not only disrupt the supply of ATP and NADPH via PSII damage but also directly inhibit key enzymes including RubisCO involved in the Calvin cycle [70,71]. Because the ^{14}C incubations were conducted without UVR, this reduction should be interpreted as post-exposure impairment rather than direct UVR inhibition during the assay. However, direct quantification of ROS and antioxidant enzyme activities, as well as lipid peroxidation products (e.g., malondialdehyde), would substantially strengthen the mechanistic interpretation. Future studies incorporating these biochemical parameters are encouraged to establish causal links between UVR exposure and oxidative stress.

In the present work, the enhancing effects of elevated pCO_2 on the strain *Synechococcus* XM24 were diminished or offset by exposures to UVR (Figure 1), reversing the responses of cellular POC and PON to pCO_2 rise (Figure 7). This indicates a substantial UVR-induced shift in resource allocation away from bulk carbon and nitrogen assimilation towards maintenance and repair processes, leaving less energy available for growth and biomass accumulation. We acknowledge that our results were based on a single coastal strain of *Synechococcus*, and that its responses to OA and UVR may differ from other strains or ecotypes. Therefore, our findings should be interpreted as a strain-specific physiological response rather than as a general response of the genus *Synechococcus*. In contrast to our results, the oceanic strain *Synechococcus* WH7803 increased its growth rate at elevated pCO_2 levels under limiting light conditions [41], whereas the coastal strain CB0101 grew slower under the elevated pCO_2 due to synergistic impacts of pH drop and high light stress [42]. While different strains of *Synechococcus* may respond differently to OA and/or UVR stress, our results about the strain XM24 from the coastal water of the East China Sea reflect that the positive effect of elevated pCO_2 could be modulated by UVR exposures. Based on the findings on *Synechococcus* strains, the pelagic WH7803 [41], coastal CB0101 [42] and XM24 (this work), it can be holistically considered that *Synechococcus* strains generally benefit less from increased CO_2 availability

when exposed to high light and/or UVR. This implies that they may be harmed in the surface oceans but benefit from increased pCO_2 in low-light environments, such as at deeper depths or under cloudy weathers. Future studies comparing multiple strains, particularly across different ecotypes such as high-light- and low-light-adapted lineages, are needed to evaluate how general the interactive effects observed here are and to better predict the response of natural *Synechococcus* populations to multiple drivers.

Supplementary Materials: The following supporting information can be downloaded at: https://www.mdpi.com/article/10.3390/phycology6040118/s1. Figure S1: The average diurnal change in solar RAR, UV-A, and UV-B near the sea surface of the coastal waters of Xiamen (Fujian province, China) during July, 2024; Figure S2: The rapid light curves of *Synechococcus* XM24 acclimated for 17 days to the growth conditions with or without periodic exposure to UVR under two CO2 levels; Figure S3: Comparison of absorption spectra in cyanobacteria *Trichodesmium* and *Synechococcus*.

Author Contributions: H.L.: Data Curation, Formal Analysis, Investigation, Project Administration, Writing—Original Draft, Writing—Review & Editing. Y.R.: Formal Analysis, Investigation, Methodology. J.C.: Data Curation, Investigation. K.G.: Conceptualization, Funding Acquisition, Methodology, Project Administration, Writing—Review & Editing. All authors have read and agreed to the published version of the manuscript.

Funding: The study was supported by the National Natural Science Foundation of China (42361144840 and 41720104005) to KSG, and the Scientific Research Foundation Program of Jiangsu Ocean University (KQ24043), and Supported by Open-end Funds of the Jiangsu Key Laboratory of Marine Bioresources and Environment (SH20231211) to HL.

Data Availability Statement: Data will be made available on request.

Acknowledgments: The authors are grateful to Rui Zhang from the Institute for Advanced Study Shenzhen University for providing the *Synechococcus* strain, and to the laboratory engineers Xianglan Zeng and Wenyan Zhao for their logistical and technical support.

Conflicts of Interest: The authors declare no conflicts of interest.

References

1. Farrant, G.K.; Doré, H.; Cornejo-Castillo, F.M.; Partensky, F.; Ratin, M.; Ostrowski, M.; Pitt, F.D.; Wincker, P.; Scanlan, D.J.; Iudicone, D. Delineating ecologically significant taxonomic units from global patterns of marine picocyanobacteria. *Proc. Natl. Acad. Sci. USA* **2016**, *113*, E3365–E3374. https://doi.org/10.1073/pnas.1524865113.
2. Callieri, C. *Synechococcus* plasticity under environmental changes. *FEMS Microbiol. Lett.* **2017**, *364*, fnx229. https://doi.org/10.1093/femsle/fnx229.
3. Flombaum, P.; Gallegos, J.L.; Gordillo, R.A.; Rincón, J.; Zabala, L.L.; Jiao, N.; Karl, D.M.; Li, W.K.; Lomas, M.W.; Veneziano, D. Present and future global distributions of the marine Cyanobacteria *Prochlorococcus* and *Synechococcus*. *Proc. Natl. Acad. Sci. USA* **2013**, *110*, 9824–9829. https://doi.org/10.1073/pnas.1307701110.
4. Garcia-Pichel, F. A model for internal self-shading in planktonic organisms and its implications for the usefulness of ultraviolet sunscreens. *Limnol. Oceanogr.* **1994**, *39*, 1704–1717. https://doi.org/10.4319/lo.1994.39.7.1704.
5. Williamson, C.E.; Zepp, R.G.; Lucas, R.M.; Madronich, S.; Austin, A.T.; Ballaré, C.L.; Norval, M.; Sulzberger, B.; Bais, A.F.; McKenzie, R.L. Solar ultraviolet radiation in a changing climate. *Nat. Clim. Change* **2014**, *4*, 434–441. https://doi.org/10.1038/nclimate2225.
6. Neale, R.E.; Barnes, P.W.; Robson, T.M.; Neale, P.J.; Williamson, C.E.; Zepp, R.G.; Wilson, S.R.; Madronich, S.; Andrady, A.L.; Heikkilä, A.M. Environmental effects of stratospheric ozone depletion, UV radiation, and interactions with climate change: UNEP Environmental Effects Assessment Panel, Update 2020. *Photochem. Photobiol. Sci.* **2021**, *20*, 1–67. https://doi.org/10.1007/s43630-020-00001-x.
7. Häder, D.-P.; Gao, K. Interactions of anthropogenic stress factors on marine phytoplankton. *Front. Environ. Sci.* **2015**, *3*, 14. https://doi.org/10.3389/fenvs.2015.00014.

8. Rastogi, R.P.; Richa, N.; Kumar, A.; Tyagi, M.B.; Sinha, R.P. Molecular mechanisms of ultraviolet radiation-induced DNA damage and repair. *J. Nucleic Acids* **2010**, *2010*, 592980. https://doi.org/10.4061/2010/592980.
9. Smith, R.C.; Cullen, J.J. Effects of UV radiation on phytoplankton. *Rev. Geophys.* **1995**, *33*, 1211–1223. https://doi.org/10.1029/95RG00801.
10. Kataria, S.; Jajoo, A.; Guruprasad, K.N. Impact of increasing Ultraviolet-B (UV-B) radiation on photosynthetic processes. *J. Photochem. Photobiol. B Biol.* **2014**, *137*, 55–66. https://doi.org/10.1016/j.jphotobiol.2014.02.004.
11. Vass, I. Molecular mechanisms of photodamage in the Photosystem II complex. *Biochim. Biophys. Acta (BBA)-Bioenerg.* **2012**, *1817*, 209–217. https://doi.org/10.1016/j.bbabio.2011.04.014.
12. Barbieri, E.S.; Villafanñ, V.E.; Helbling, E.W. Experimental assessment of UV effects on temperate marine phytoplankton when exposed to variable radiation regimes. *Limnol. Oceanogr.* **2002**, *47*, 1648–1655. https://doi.org/10.4319/lo.2002.47.6.1648.
13. Villafane, V.E.; Gao, K.; Li, P.; Li, G.; Walter Helbling, E. Vertical mixing within the epilimnion modulates UVR-induced photoinhibition in tropical freshwater phytoplankton from southern China. *Freshw. Biol.* **2007**, *52*, 1260–1270. https://doi.org/10.1111/j.1365-2427.2007.01762.x.
14. Gao, K.; Wu, Y.; Li, G.; Wu, H.; Villafane, V.E.; Helbling, E.W. Solar UV radiation drives CO_2 fixation in marine phytoplankton: A double-edged sword. *Plant Physiol.* **2007**, *144*, 54–59. https://doi.org/10.1104/pp.107.098491.
15. Jin, P.; Gao, K.; Villafañe, V.E.; Campbell, D.A.; Helbling, E.W. Ocean acidification alters the photosynthetic responses of a coccolithophorid to fluctuating ultraviolet and visible radiation. *Plant Physiol.* **2013**, *162*, 2084–2094. https://doi.org/10.1104/pp.113.219543.
16. Rastogi, R.P.; Sinha, R.P.; Moh, S.H.; Lee, T.K.; Kottuparambil, S.; Kim, Y.-J.; Rhee, J.-S.; Choi, E.-M.; Brown, M.T.; Häder, D.-P. Ultraviolet radiation and cyanobacteria. *J. Photochem. Photobiol. B Biol.* **2014**, *141*, 154–169. https://doi.org/10.1016/j.jphotobiol.2014.09.020.
17. Häder, D.-P.; Williamson, C.E.; Wängberg, S.-Å.; Rautio, M.; Rose, K.C.; Gao, K.; Helbling, E.W.; Sinha, R.P.; Worrest, R. Effects of UV radiation on aquatic ecosystems and interactions with other environmental factors. *Photochem. Photobiol. Sci.* **2015**, *14*, 108–126. https://doi.org/10.1039/C4PP90035A.
18. Singh, V.K.; Jha, S.; Rana, P.; Mishra, S.; Kumari, N.; Singh, S.C.; Anand, S.; Upadhye, V.; Sinha, R.P. Resilience and mitigation strategies of cyanobacteria under ultraviolet radiation stress. *Int. J. Mol. Sci.* **2023**, *24*, 12381, doi:doi.org/10.3390/ijms241512381.
19. Guan, W.; Gao, K. Impacts of UV radiation on photosynthesis and growth of the coccolithophore *Emiliania huxleyi* (Haptophyceae). *Environ. Exp. Bot.* **2010**, *67*, 502–508. https://doi.org/10.1016/j.envexpbot.2009.08.003.
20. Haney, A.M.; Sanfilippo, J.E.; Garczarek, L.; Partensky, F.; Kehoe, D.M. Multiple photolyases protect the marine cyanobacterium *Synechococcus* from ultraviolet radiation. *Mbio* **2022**, *13*, e01511-01522, doi:doi.org/10.1128/mbio.01511-22.
21. Halac, S.R.; Villafañe, V.E.; Helbling, E.W. Temperature benefits the photosynthetic performance of the diatoms *Chaetoceros gracilis* and *Thalassiosira weissflogii* when exposed to UVR. *J. Photochem. Photobiol. B Biol.* **2010**, *101*, 196–205. https://doi.org/10.1016/j.jphotobiol.2010.07.003.
22. García-Gómez, C.; Gordillo, F.J.; Palma, A.; Lorenzo, M.R.; Segovia, M. Elevated CO_2 alleviates high PAR and UV stress in the unicellular chlorophyte *Dunaliella tertiolecta*. *Photochem. Photobiol. Sci.* **2014**, *13*, 1347–1358. https://doi.org/10.1039/C4PP00044G.
23. Jiang, X.; Zhang, Y.; Hutchins, D.A.; Gao, K. Nitrogen-limitation exacerbates the impact of ultraviolet radiation on the coccolithophore *Gephyrocapsa oceanica*. *J. Photochem. Photobiol. B Biol.* **2022**, *226*, 112368. https://doi.org/10.1016/j.jphotobiol.2021.112368.
24. Heraud, P.; Roberts, S.; Shelly, K.; Beardall, J. Interactions between UV-B exposure and phosphorus nutrition. II. effects on rates of damage and repair. *J. Phycol.* **2005**, *41*, 1212–1218. https://doi.org/10.1111/j.1529-8817.2005.00149.x.
25. Buma, A.G.; Helbling, E.W.; de Boer, M.K.; Villafane, V.E. Patterns of DNA damage and photoinhibition in temperate South-Atlantic picophytoplankton exposed to solar ultraviolet radiation. *J. Photochem. Photobiol. B Biol.* **2001**, *62*, 9–18. https://doi.org/10.1016/S1011-1344(01)00156-7.
26. Llabrés, M.; Agustí, S. Picophytoplankton cell death induced by UV radiation: Evidence for oceanic Atlantic communities. *Limnol. Oceanogr.* **2006**, *51*, 21–29. https://doi.org/10.4319/lo.2006.51.1.0021.
27. Neale, P.; Pritchard, A.; Ihnacik, R. UV effects on the primary productivity of picophytoplankton: Biological weighting functions and exposure response curves of *Synechococcus*. *Biogeosciences* **2014**, *11*, 2883–2895. https://doi.org/10.5194/bg-11-2883-2014.
28. Fragoso, G.M.; Neale, P.J.; Kana, T.M.; Pritchard, A.L. Kinetics of photosynthetic response to ultraviolet and photosynthetically active radiation in *Synechococcus* WH8102 (*Cyanobacteria*). *Photochem. Photobiol.* **2014**, *90*, 522–532. https://doi.org/10.1111/php.12202.

29. Six, C.; Joubin, L.; Partensky, F.; Holtzendorff, J.; Garczarek, L. UV-induced phycobilisome dismantling in the marine picocyanobacterium *Synechococcus* sp. WH8102. *Photosynth. Res.* **2007**, *92*, 75–86. https://doi.org/10.1007/s11120-007-9170-4.
30. Yi, X.; Gao, K. Impact of ultraviolet radiation nearly overrides the effects of elevated pCO_2 on a prominent nitrogen-fixing cyanobacterium. *Limnol. Oceanogr.* **2023**, *68*, 557–568. https://doi.org/10.1002/lno.12294.
31. Gattuso, J.-P.; Magnan, A.; Billé, R.; Cheung, W.W.; Howes, E.L.; Joos, F.; Allemand, D.; Bopp, L.; Cooley, S.R.; Eakin, C.M. Contrasting futures for ocean and society from different anthropogenic CO_2 emissions scenarios. *Science* **2015**, *349*, aac4722. https://doi.org/10.1126/science.aac4722.
32. Cai, W.-J.; Hu, X.; Huang, W.-J.; Murrell, M.C.; Lehrter, J.C.; Lohrenz, S.E.; Chou, W.-C.; Zhai, W.; Hollibaugh, J.T.; Wang, Y. Acidification of subsurface coastal waters enhanced by eutrophication. *Nat. Geosci.* **2011**, *4*, 766–770. https://doi.org/10.1038/ngeo1297.
33. Feely, R.A.; Alin, S.R.; Newton, J.; Sabine, C.L.; Warner, M.; Devol, A.; Krembs, C.; Maloy, C. The combined effects of ocean acidification, mixing, and respiration on pH and carbonate saturation in an urbanized estuary. *Estuar. Coast. Shelf Sci.* **2010**, *88*, 442–449. https://doi.org/10.1016/j.ecss.2010.05.004.
34. Gao, K.; Campbell, D.A. Photophysiological responses of marine diatoms to elevated CO_2 and decreased pH: A review. *Funct. Plant Biol.* **2014**, *41*, 449–459. https://doi.org/10.1071/FP13247.
35. Hong, H.; Shen, R.; Zhang, F.; Wen, Z.; Chang, S.; Lin, W.; Kranz, S.A.; Luo, Y.-W.; Kao, S.-J.; Morel, F.M. The complex effects of ocean acidification on the prominent N_2-fixing cyanobacterium Trichodesmium. *Science* **2017**, *356*, 527–531. https://doi.org/10.1126/science.aal2981.
36. Gao, K.; Xu, J.; Gao, G.; Li, Y.; Hutchins, D.A.; Huang, B.; Wang, L.; Zheng, Y.; Jin, P.; Cai, X. Rising CO_2 and increased light exposure synergistically reduce marine primary productivity. *Nat. Clim. Change* **2012**, *2*, 519–523. https://doi.org/10.1038/nclimate1507.
37. Li, Y.; Gao, K.; Villafañe, V.E.; Helbling, E.W. Ocean acidification mediates photosynthetic response to UV radiation and temperature increase in the diatom *Phaeodactylum tricornutum*. *Biogeosciences* **2012**, *9*, 3931–3942. https://doi.org/10.5194/bg-9-3931-2012.
38. Gao, K.; Beardall, J.; Häder, D.-P.; Hall-Spencer, J.M.; Gao, G.; Hutchins, D.A. Effects of ocean acidification on marine photosynthetic organisms under the concurrent influences of warming, UV radiation, and deoxygenation. *Front. Mar. Sci.* **2019**, *6*, 322. https://doi.org/10.3389/fmars.2019.00322.
39. Häder, D.-P.; Gao, K. Aquatic productivity under multiple stressors. *Water* **2023**, *15*, 817, doi:doi.org/10.3390/w15040817.
40. Boyd, P.W.; Collins, S.; Dupont, S.; Fabricius, K.; Gattuso, J.P.; Havenhand, J.; Hutchins, D.A.; Riebesell, U.; Rintoul, M.S.; Vichi, M. Experimental strategies to assess the biological ramifications of multiple drivers of global ocean change—A review. *Glob. Change Biol.* **2018**, *24*, 2239–2261. https://doi.org/10.1111/gcb.14102.
41. Bao, N.; Gao, K. Interactive effects of elevated CO_2 concentration and light on the picophytoplankton *Synechococcus*. *Front. Mar. Sci.* **2021**, *8*, 634189. https://doi.org/10.3389/fmars.2021.634189.
42. Li, H.; Beardall, J.; Gao, K. Photoinhibition of the picophytoplankter *Synechococcus* is exacerbated by ocean acidification. *Water* **2023**, *15*, 1228. https://doi.org/10.3390/w15061228.
43. Guyet, U.; Nguyen, N.A.; Doré, H.; Haguait, J.; Pittera, J.; Conan, M.; Ratin, M.; Corre, E.; Le Corguillé, G.; Brillet-Guéguen, L. Synergic effects of temperature and irradiance on the physiology of the marine *Synechococcus* strain WH7803. *Front. Microbiol.* **2020**, *11*, 1707. https://doi.org/10.3389/fmicb.2020.01707.
44. Zhou, L.; Gao, S.; Yang, W.; Wu, S.; Huan, L.; Xie, X.; Wang, X.; Lin, S.; Wang, G. Transcriptomic and metabolic signatures of diatom plasticity to light fluctuations. *Plant Physiol.* **2022**, *190*, 2295–2314. https://doi.org/10.1093/plphys/kiac455.
45. Waterbury, J.B. Biological and ecological characterization of the marine unicellular cyanobacterium *Synechococcus*. *Can Bull. Fish Aquat. Sci.* **1986**, *214*, 71–120.
46. Gao, K. Approaches and involved principles to control pH/pCO_2 stability in algal cultures. *J. Appl. Phycol.* **2021**, *33*, 3497–3505. https://doi.org/10.1007/s10811-021-02585-y.
47. Marie, D.; Partensky, F.; Vaulot, D.; Brussaard, C. Enumeration of phytoplankton, bacteria, and viruses in marine samples. *Curr. Protoc. Cytom.* **1999**, *10*, 11.11.11–11.11.15. https://doi.org/10.1002/0471142956.cy1111s10.
48. Ritchie, R.J. Consistent sets of spectrophotometric chlorophyll equations for acetone, methanol and ethanol solvents. *Photosynth. Res.* **2006**, *89*, 27–41. https://doi.org/10.1007/s11120-006-9065-9.
49. Wellburn, A.R. The spectral determination of chlorophylls a and b, as well as total carotenoids, using various solvents with spectrophotometers of different resolution. *J. Plant Physiol.* **1994**, *144*, 307–313. https://doi.org/10.1016/S0176-1617(11)81192-2.

50. Villafañe, V.E.; Helbling, E.W.; Holm-Hansen, O.; Chalker, B.E. Acclimatization of Antarctic natural phytoplankton assemblages when exposed to solar ultraviolet radiation. *J. Plankton Res.* **1995**, *17*, 2295–2306. https://doi.org/10.1093/plankt/17.12.2295.
51. Eilers, P.; Peeters, J. A model for the relationship between light intensity and the rate of photosynthesis in phytoplankton. *Ecol. Model.* **1988**, *42*, 199–215. https://doi.org/10.1016/0304-3800(88)90057-9.
52. Heraud, P.; Beardall, J. Changes in chlorophyll fluorescence during exposure of *Dunaliella tertiolecta* to UV radiation indicate a dynamic interaction between damage and repair processes. *Photosynth. Res.* **2000**, *63*, 123–134. https://doi.org/10.1023/A:1006319802047.
53. Marcoval, M.A.; Villafañe, V.E.; Helbling, E.W. Interactive effects of ultraviolet radiation and nutrient addition on growth and photosynthesis performance of four species of marine phytoplankton. *J. Photochem. Photobiol. B Biol.* **2007**, *89*, 78–87. https://doi.org/10.1016/j.jphotobiol.2007.09.004.
54. Zhu, Z.; Fu, F.; Qu, P.; Mak, E.W.K.; Jiang, H.; Zhang, R.; Zhu, Z.; Gao, K.; Hutchins, D.A. Interactions between ultraviolet radiation exposure and phosphorus limitation in the marine nitrogen-fixing cyanobacteria *Trichodesmium* and *Crocosphaera*. *Limnol. Oceanogr.* **2020**, *65*, 363–376. https://doi.org/10.1002/lno.11304.
55. Kumar, V.; Mondal, S.; Gupta, A.; Maurya, P.K.; Sinha, R.P.; Häder, D.-P.; Singh, S.P. Light-dependent impact of salinity on the ecophysiology of *Synechococcus elongatus* PCC 7942: Genetic and comparative protein structure analyses of UV-absorbing mycosporine-like amino acids (MAAs) biosynthesis. *Environ. Exp. Bot.* **2021**, *191*, 104620. https://doi.org/10.1016/j.envexpbot.2021.104620.
56. Singh, S.P.; Klisch, M.; Sinha, R.P.; Häder, D.-P. Genome mining of mycosporine-like amino acid (MAA) synthesizing and non-synthesizing cyanobacteria: A bioinformatics study. *Genomics* **2010**, *95*, 120–128. https://doi.org/10.1016/j.ygeno.2009.10.002.
57. Castenholz, R.W.; Garcia-Pichel, F. Cyanobacterial responses to UV radiation. In *Ecology of Cyanobacteria II: Their Diversity in Space and Time*; Springer: Berlin/Heidelberg, Germany, 2012, pp. 481–499.
58. Sass, L.; Spetea, C.; Máté, Z.; Nagy, F.; Vass, I. Repair of UV-B induced damage of Photosystem II via *de novo* synthesis of the D1 and D2 reaction centre subunits in *Synechocystis* sp. PCC 6803. *Photosynth. Res.* **1997**, *54*, 55–62. https://doi.org/10.1023/A:1005895924892.
59. Price, G.D.; Badger, M.R.; Woodger, F.J.; Long, B.M. Advances in understanding the cyanobacterial CO_2-concentrating-mechanism (CCM): Functional components, Ci transporters, diversity, genetic regulation and prospects for engineering into plants. *J. Exp. Bot.* **2008**, *59*, 1441–1461. https://doi.org/10.1093/jxb/erm112.
60. Sharbaugh, A.K.; Laws, E.A. Interactive effects of CO_2, temperature, and nitrate limitation on the growth and physiology of strain CCMP 1334 of the marine cyanobacterium *Synechococcus* (*Cyanophyceae*). *J. Phycol.* **2025**, *61*, 77–90. https://doi.org/10.1111/jpy.13531.
61. Vila, X.; Abella, C.A. Light-harvesting adaptations of planktonic phototrophic micro-organisms to different light quality conditions. *Hydrobiologia* **2001**, *452*, 15–30. https://doi.org/10.1023/A:1011909330390.
62. Tan, Y.-H.; Poong, S.-W.; Yang, C.-H.; Lim, P.-E.; John, B.; Pai, T.-W.; Phang, S.-M. Transcriptomic analysis reveals distinct mechanisms of adaptation of a polar picophytoplankter under ocean acidification conditions. *Mar. Environ. Res.* **2022**, *182*, 105782. https://doi.org/10.1016/j.marenvres.2022.105782.
63. Sabia, A.; Clavero, E.; Pancaldi, S.; Salvado Rovira, J. Effect of different CO_2 concentrations on biomass, pigment content, and lipid production of the marine diatom *Thalassiosira pseudonana*. *Appl. Microbiol. Biotechnol.* **2018**, *102*, 1945–1954. https://doi.org/10.1007/s00253-017-8728-0.
64. Bhatti, A.F.; Kirilovsky, D.; van Amerongen, H.; Wientjes, E. State transitions and photosystems spatially resolved in individual cells of the cyanobacterium *Synechococcus elongatus*. *Plant Physiol.* **2021**, *186*, 569–580. https://doi.org/10.1093/plphys/kiab063.
65. Pathak, J.; Häder, D.-P.; Sinha, R.P. Impacts of ultraviolet radiation on certain physiological and biochemical processes in cyanobacteria inhabiting diverse habitats. *Environ. Exp. Bot.* **2019**, *161*, 375–387. https://doi.org/10.1016/j.envexpbot.2018.10.037.
66. Xie, L.; Macken, A.; Tollefsen, K.E. Interactive effects of elevated atmospheric CO_2 and UV-B radiation: A multi-level study on marine diatom *Skeletonema pseudocostatum*. *Ecotoxicol. Environ. Saf.* **2025**, *291*, 117879. https://doi.org/10.1016/j.ecoenv.2025.117879.
67. Edge, R.; McGarvey, D.; Truscott, T. The carotenoids as anti-oxidants—A review. *J. Photochem. Photobiol. B Biol.* **1997**, *41*, 189–200. https://doi.org/10.1016/S1011-1344(97)00092-4.
68. Singh, S.; Rastogi, R.; Sinha, R.; Häder, D.-P. Photosynthetic performance of *Anabaena variabilis* PCC 7937 under simulated solar radiation. *Photosynthetica* **2013**, *51*, 259–266. https://doi.org/10.1007/s11099-013-0012-7.

69. Wu, H.; Abasova, L.; Cheregi, O.; Deák, Z.; Gao, K.; Vass, I. D1 protein turnover is involved in protection of Photosystem II against UV-B induced damage in the cyanobacterium *Arthrospira* (Spirulina) *platensis*. *J. Photochem. Photobiol. B Biol.* **2011**, *104*, 320–325. https://doi.org/10.1016/j.jphotobiol.2011.01.004.
70. Bouchard, J.; Longhi, M.; Roy, S.; Campbell, D.; Ferreyra, G. Interaction of nitrogen status and UVB sensitivity in a temperate phytoplankton assemblage. *J. Exp. Mar. Biol. Ecol.* **2008**, *359*, 67–76. https://doi.org/10.1016/j.jembe.2008.02.022.
71. Sinha, R.; Singh, N.; Kumar, A.; Kumar, H.; Häder, M.; Häder, D.-P. Effects of UV irradiation on certain physiological and biochemical processes in cyanobacteria. *J. Photochem. Photobiol. B Biol.* **1996**, *32*, 107–113. https://doi.org/10.1016/1011-1344(95)07205-5.

Disclaimer/Publisher's Note: The statements, opinions and data contained in all publications are solely those of the individual author(s) and contributor(s) and not of MDPI and/or the editor(s). MDPI and/or the editor(s) disclaim responsibility for any injury to people or property resulting from any ideas, methods, instructions or products referred to in the content.